*Int. J. Urban Manage. Energy Sustainability, 7(1):305-315, 2026*

International Journal of Urban Management and Energy Sustainability (IJUMES)

Homepage: http://www.ijumes.com

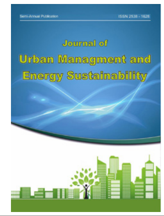


CASE STUDY RESEARCH PAPER

# Optimization of CFST Column Parameters Employing the Taguchi Method and Finite Element Analysis

Masoud Azimi, Mohammad Reza Habibi*, Mohammad Hadi Tavana

*Department of Engineering, Ker.C., Islamic Azad University, Kermanshah, Iran*

ARTICLE INFO

*Article History:*
Received 2026-02-02
Revised 2026-04-25
Accepted 2026-05-20

*Keywords:*
ANSYS software; CFST column; Finite element analysis; optimization; Taguchi method

ABSTRACT

Concrete-filled steel tubular (CFST) columns combine the complementary advantages of steel and concrete and are increasingly used as axial-load-carrying members in high-rise and seismic-resistant construction. Problem statement: Because the structural quality of a CFST column depends on several interacting geometric and material parameters, and because full experimental programmes are costly, there is a need for a systematic, economical procedure to identify the parameter combination that optimises column performance. This study determines the optimal construction parameters of a circular CFST column so as to minimise elastic-stiffness loss and von Mises failure stress while maximising load resistance, fatigue resistance and service life by combining finite-element analysis with the Taguchi design of experiments. A CFST column was modelled and solved by the finite-element method in ANSYS. Four control parameters, each at three levels, were arranged in a Taguchi L9 orthogonal array; the resulting nine models were analysed in two loading series, giving the maximum displacement and the maximum von Mises stress, and the responses were evaluated through signal-to-noise (S/N) ratios and mean-effect analysis in Minitab. Stirrup spacing, concrete grade and plate thickness significantly affected column quality, whereas the reinforcement material was almost ineffective. The optimal combination was A2B2C3D1, a 6 cm stirrup spacing, the intermediate plate thickness, 35 MPa concrete and steel reinforcement which produced the lowest von Mises stress and the lowest probability of failure and buckling. The integrated Taguchi–finite-element approach efficiently identifies the parameters that govern CFST-column quality and provides a validated, economical route to optimal composite-column design.

DOI: 10.22034/ijumes.2026.2096172.1386

*Running Title: CFST Column Parameters Employing the Taguchi Method and Finite Element Analysis*

| NUMBER OF REFERENCES | NUMBER OF FIGURES | NUMBER OF TABLES |
|---|---|---|
| 40 | 08 | 07 |

*Corresponding Author:
Email: *m.r.habibi@iau.ac.ir*
*Phone: +988337243181*
ORCID: https://orcid.org/0000-0001-7559-4788

## INTRODUCTION

Owing to the abundant benefits of concrete-filled steel tubular (CFST) columns a type of composite column compared with reinforced-concrete and steel columns, their use has become widespread in recent years, particularly in high-rise buildings. Ease of installation, economy, elimination of formwork, good performance against seismic forces, and higher strength and ductility at lower volume are among these benefits (Han et al., 2014; Schneider, 1998). A CFST column is a steel–concrete composite member consisting of a steel tube filled with high-strength concrete, whose favourable behaviour arises from the confinement of the concrete by the steel and from its design versatility. Its principal cross-sections are square, rectangular and circular; columns designed so that the concrete resists most of the axial force can be made more economical with a thin-walled steel tube. The outstanding static and earthquake-resistant properties of rectangular and circular CFST member's high strength, ductility and energy-absorption capacity explain their extensive use in civil-engineering projects (Shanmugam & Lakshmi, 2001). When applied as structural columns, especially in tall buildings, composite members may be subjected to high shear forces and moments under wind or seismic actions. This study investigates the strengthening of a composite concrete column enclosed in a steel plate with composite reinforcements. The stress–strain diagram of structural mild steel is introduced multi-linearly into the software to capture material non-linearity, and the effects of pre-loading, inner and outer plate buckling and large deformation are considered for greater analytical accuracy; the numerical results are compared with reliable experimental data. Considerable attention is paid to the analytical approach of conducting software-simulated experiments by the finite-element method in ANSYS, after which the Taguchi method with orthogonal arrays is used to evaluate the optimal operating conditions of the CFST column a systematic approach to designing and analysing experiments that allows the effect of each parameter to be assessed independently (Lee & Wong, 2023; Anwar et al., 2022).

The concept of hybrid columns comprising two concentric steel layers with concrete enclosed between them was first proposed by Shakir-Khalil and Illouli (Shakir-Khalil & Illouli, 1987), and subsequent studies extended the idea in various directions (Wei et al., 1995; Han et al., 2005; Zhao & Grzebieta, 2002; Tao et al., 2004). The stress–strain behaviour of double-skin tubular columns and the wet-layup application of fibre-reinforced-polymer (FRP) layers were examined by Yu and colleagues (Yu et al., 2010), while the steel-jacket strengthening of reinforced-concrete columns using angles, C-sections and plates of various sizes and batten-plate numbers was investigated experimentally and by finite-element modelling in ANSYS, with good agreement between the two (Belal et al., 2014). Analytical models for the axial capacity of concrete-encased steel composite stub columns, incorporating the confinement effect through the Mander model in ABAQUS, showed that confinement increases load-carrying capacity and that the steel-section shape and reinforcement layout are influential the cross-shaped section giving the highest confinement and the I-shaped the lowest (Chen & Lin, 2006; Mander et al., 1988). Eccentrically loaded concrete-encased steel composite columns, modelled with confined zones in ABAQUS using a plastic-damage formulation, reproduced experiments well and revealed that increasing the steel yield stress markedly affects columns with small eccentricity (Ellobody et al., 2011; Lubliner et al., 1989). Concrete-filled double-skin steel tubes (CFDST) under axial load and cyclic bending showed that circular sections dissipate more energy and are more ductile than square ones (Han et al., 2006; Zhao & Han, 2006).

Extensive research has also addressed CFST columns of different cross-sections and loading conditions. Under torsional loading the outer steel profile acts in harmony with the concrete core in the plastic phase, the concrete core governs torsional resistance, and the concrete prevents local buckling of the steel profile (Zhou, 1990; Beck & Kiyomiya, 2003); empirical and analytical studies of CFDST columns further confirmed these composite benefits (Zhao et al., 2002; Wei et al., 1995). Reinforced-concrete square columns retrofitted with stirrups and steel angles (steel cage) were tested to failure, identifying the angle size, stirrup spacing and grout material as the principal parameters (Tarabia & Albakry, 2014). Recent work has extended CFST research to FRP-confined, recycled-aggregate and seawater sea-sand columns, and to advanced finite-element modelling of their axial behaviour (Zeng et al., 2022; Liang et al., 2021; Liang et al., 2023; Liao et al., 2023; Li et al., 2024; Al-Rousan et al., 2022).

Despite this extensive body of work, most studies vary one parameter at a time or rely on large experimental programmes, which is costly and does not reveal the relative importance of the interacting design variables. Design-of-experiments techniques such as the Taguchi method, widely applied to concrete-mix and composite-material optimisation (Anwar et al., 2022; Zamir Hashmi et al., 2022; Lee & Wong, 2023), remain comparatively underused for the parametric optimisation of CFST columns through validated finite-element models. The present study addresses this gap by coupling ANSYS finite-element analysis with a Taguchi L9 design to rank the governing parameters and identify the optimal CFST-column configuration. Two questions guide the work: which construction parameters most strongly influence the quality (stiffness and von Mises failure response) of a circular CFST column, and what combination of their levels yields the optimal performance? The purpose of this study is to obtain the optimal dimensional and material parameters for constructing a circular CFST column, so as to achieve the best quality levels, by combining finite-element analysis in ANSYS with the Taguchi design of experiments. Four control parameters stirrup spacing, plate thickness, concrete grade and reinforcement material, each at three levels are examined through an L9 orthogonal array, and the optimal combination is identified from the S/N and mean-effect analyses.

## MATERIALS AND METHODS

### *Design and finite-element model*

The study investigates the strengthening of a composite concrete column enclosed in a steel plate with composite reinforcements. The stress–strain curve of structural mild steel is introduced multi-linearly into ANSYS to represent material non-linearity, and the effects of pre-loading, inner and outer plate buckling, and large deformation are included for accuracy. Each specimen has nominal dimensions defined by the section diameter D, the steel-wall thickness t and the tube height H. The top view of the studied models is shown in Figure 1. In the finite-element model, the steel tube and reinforcement were represented by an elastic–plastic constitutive law with a multi-linear hardening stress–strain curve, while the confined concrete core was represented by a plasticity-based model that captures the triaxial confinement provided by the steel tube (Mander et al., 1988; Lubliner et al., 1989). A surface-to-surface contact with appropriate normal and tangential behaviour was defined at the steel–concrete interface, and the loading was applied incrementally to trace the non-linear response up to failure. This modelling strategy follows current practice for CFST members and allows local buckling of the tube and confinement-induced stress redistribution in the concrete to be reproduced (Li et al., 2024; Han et al., 2014). (Fig. 1)

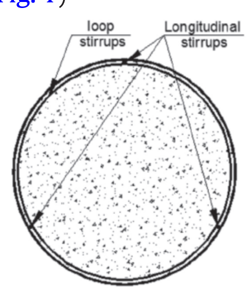


Figure 1: Top view of the CFST column models studied in this research

*Verification of the simulated model*

To verify the ANSYS results, a laboratory model of a concrete column enclosed by a steel plate and stirrups was selected and its response compared with the finite-element model. The slight difference between the experimental and analytical results confirms the accuracy of the modelling. The experimental and numerical models used for the accuracy evaluation are shown in Figure 2. (Fig. 2 and 3)

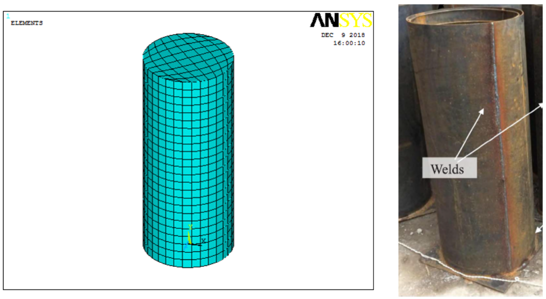


Figure 2: Numerical model (left) and experimental specimen (right) used for the accuracy evaluation

*Determining target quality levels and possible effective parameters*

Following a brainstorming session, four control parameters affecting the quality of the CFST column were selected, each at three levels: stirrup spacing (A), steel-plate thickness (B), concrete grade (C) and reinforcement material (D). The expected quality responses were a controlled reduction of the elastic stiffness of the column, an increased pressure tolerance over the whole member, fatigue resistance and long service life. The total number of degrees of freedom indicated that at least nine experiments were required, so the tests were arranged in a Taguchi L9 orthogonal array; considering the three levels across the models, 81 specimen states were effectively examined and the optimum selected through the Taguchi algorithm. The factors and their levels are listed in Table 1, and the L9 design in Table 2. (Tab. 1 and 2)

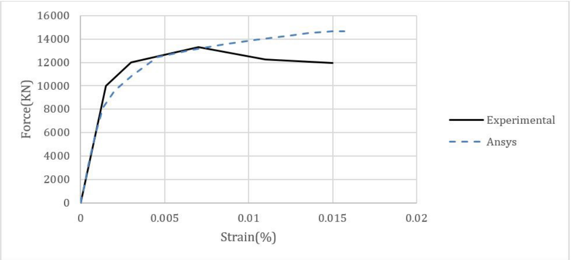


Figure 3: Comparison plot of experimental and analytical results

Table 1: Control factors and their levels

| Level | A – stirrup spacing (cm) | B – plate thickness (mm) | C – concrete grade (MPa) | D – reinforcement |
|---|---|---|---|---|
| 1 | 5 | 2 | 25 | Steel |
| 2 | 6 | 4 | 30 | CFRP |
| 3 | 8 | 6 | 35 | GFRP |

Table 2: Taguchi L9 orthogonal-array design with the actual factor values

| Test | A | B | C | D |
|---|---|---|---|---|
| 1 | 5 cm | 2 mm | 25 MPa | Steel |
| 2 | 5 cm | 4 mm | 30 MPa | CFRP |
| 3 | 5 cm | 6 mm | 35 MPa | GFRP |
| 4 | 6 cm | 2 mm | 30 MPa | GFRP |
| 5 | 6 cm | 4 mm | 35 MPa | Steel |
| 6 | 6 cm | 6 mm | 25 MPa | CFRP |
| 7 | 8 cm | 2 mm | 35 MPa | CFRP |

| | | | | |
|---|---|---|---|---|
| 8 | 8 cm | 4 mm | 25 MPa | GFRP |
| 9 | 8 cm | 6 mm | 30 MPa | Steel |

*Von Mises criterion*

The maximum-distortion-energy (von Mises) yield criterion, proposed by von Mises in 1913, states that yielding begins when the distortion (deviatoric) component of the strain energy exceeds the value at yield in a simple tension test. Strain energy is divided into a volumetric (hydrostatic) part and a deviatoric (distortion) part; if the computed von Mises stress is below the material yield stress no failure occurs, otherwise the element yields. The von Mises stress is obtained from the principal stresses and is compared with the yield stress in the finite-element software.

$$\sigma\_v = \sqrt{ \tfrac{1}{2}[(\sigma_1-\sigma_2)^2 + (\sigma_2-\sigma_3)^2 + (\sigma_3-\sigma_1)^2] } \qquad (1)$$

*Execution of the Taguchi experiments in ANSYS*

Nine CFST-column models were simulated in ANSYS, the level of each factor being set according to the test number (1–9) of the L9 array. Each model was analysed by finite-element analysis, and the resulting solutions were processed through the signal-to-noise (S/N) ratios of the Taguchi method. The side view of the meshed model and a three-dimensional view of the meshed reinforcement are shown in Figures 3 and 4.

Two S/N ratios were used according to the desired direction of each quality characteristic. For the elastic-stiffness reduction (displacement), which should be maximised, the larger-the-better ratio was applied; for the von Mises failure stress, which should be minimised, the smaller-the-better ratio was applied:

$$\text{S/N (larger-the-better)} = -10 \log_{10} \left[ (1/n)\, \Sigma\, (1/y_i^2) \right] \qquad (2)$$

$$\text{S/N (smaller-the-better)} = -10 \log_{10} \left[ (1/n)\, \Sigma\, y_i^2 \right] \qquad (3)$$

where $y_i$ is the response of the i-th replicate and n is the number of replicates. The optimal level of each factor corresponds to the highest S/N value, and the relative importance of the factors is obtained from the range (delta) of the mean responses across their levels. (Fig. 3 and 4)

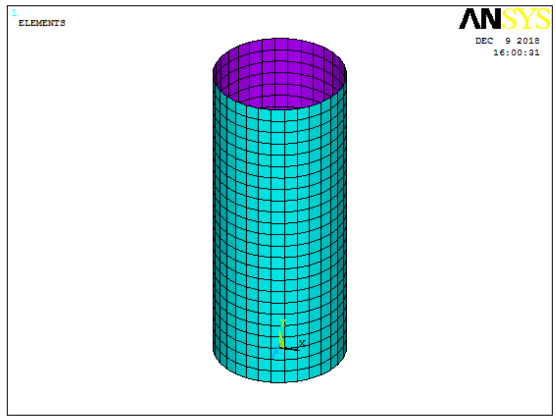


Figure 3: Side view of the meshed CFST-column model in ANSYS

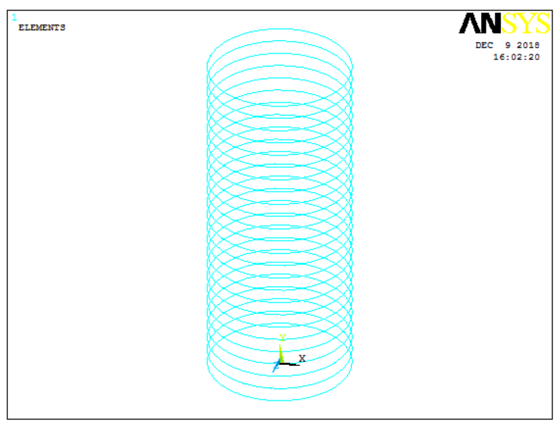


Figure 4: Three-dimensional view of the meshed reinforcement of the CFST-column model in ANSYS

## FINDINGS AND DISCUSSION

*Results of the nine tests*

Two loading series were considered: series (a), with pressure along the Z-axis, and series (b), with loading along the X-axis (column buckling).

For each of the nine tests, the finite-element analysis yielded the maximum displacement and the maximum von Mises stress. The results are summarised in Tables 3–6.

Table 3: Series (a) – maximum displacement along the Z-axis

| Test | Max. displacement, Z-axis (m) |
|---|---|
| 1 | $7.71\times10^{-3}$ |
| 2 | $7.98\times10^{-3}$ |
| 3 | $8.86\times10^{-3}$ |
| 4 | $2.00\times10^{-2}$ |
| 5 | $6.99\times10^{-3}$ |
| 6 | $8.15\times10^{-3}$ |
| 7 | $1.77\times10^{-2}$ |
| 8 | $1.67\times10^{-2}$ |
| 9 | $6.41\times10^{-3}$ |

Table 4: Series (b) – maximum displacement along the X-axis

| Test | Max. displacement, X-axis (m) |
|---|---|
| 1 | $2.18\times10^{-4}$ |
| 2 | $2.01\times10^{-4}$ |
| 3 | $1.93\times10^{-4}$ |
| 4 | $4.61\times10^{-4}$ |
| 5 | $1.69\times10^{-4}$ |
| 6 | $1.88\times10^{-4}$ |
| 7 | $4.71\times10^{-4}$ |
| 8 | $4.15\times10^{-4}$ |
| 9 | $1.58\times10^{-4}$ |

Table 5: Series (a) – maximum von Mises stress

| Test | Max. von Mises stress, series (a) (Pa) |
|---|---|
| 1 | $2.24\times10^{7}$ |
| 2 | $2.17\times10^{7}$ |
| 3 | $2.14\times10^{7}$ |
| 4 | $3.00\times10^{7}$ |
| 5 | $1.61\times10^{7}$ |
| 6 | $1.81\times10^{7}$ |
| 7 | $2.53\times10^{7}$ |
| 8 | $2.33\times10^{7}$ |
| 9 | $2.24\times10^{7}$ |

Table 6: Series (b) – maximum von Mises stress

| Test | Max. von Mises stress, series (b) (Pa) |
|---|---|
| 1 | $3.92\times10^{7}$ |
| 2 | $3.74\times10^{7}$ |
| 3 | $3.62\times10^{7}$ |
| 4 | $5.23\times10^{7}$ |
| 5 | $3.52\times10^{7}$ |
| 6 | $3.94\times10^{7}$ |
| 7 | $5.98\times10^{7}$ |
| 8 | $6.11\times10^{7}$ |
| 9 | $4.06\times10^{7}$ |

*Analysis of S/N performance ratios for experiments*

*Numerical results of S/N performance ratios for experiments*

There are three quality characteristics in this study, including strength, ductility, and energy absorption. Since the nature of solutions obtained in experiments is software, one can choose S/N ratio proportional to their nature to achieve the desired quality level in each of these two types of experiments. Therefore, we describe the concept of S/N ratios for each type of experiment in a separate section.

*Description of S/N ratio in software experiments:*

Here, the purpose of these experiments is to obtain a combination of levels of control factors so that the average value of the elastic stiffness reduction of the CFST column (the amount of displacement of the spring under compression along the Z-axis of the cylinder) should be maximized in software experiments by retaining its elasticity. Moreover, the characteristic of resistance to vertical loading and failure of the CFST column should increase under operating pressure so that the average of the measurement scale of this characteristic, i.e., the value of von Mises failure stress, should be minimized in software testing.

Table 7: Respons and levels

| Response | Level | A | B | C | D |
|---|---|---|---|---|---|
| Displacement Z | 1 | 8.183 | 15.137 | 10.853 | 7.037 |
| | 2 | 11.713 | 10.557 | 11.463 | 11.277 |
| | 3 | 13.603 | 7.807 | 11.183 | 15.187 |
| Displacement X | 1 | 0.204 | 0.383 | 0.274 | 0.182 |
| | 2 | 0.273 | 0.262 | 0.273 | 0.287 |
| | 3 | 0.348 | 0.180 | 0.278 | 0.356 |
| Von Mises (a) | 1 | 21.83 | 25.90 | 21.27 | 20.30 |
| | 2 | 21.40 | 20.37 | 24.70 | 21.70 |
| | 3 | 23.67 | 20.63 | 20.93 | 24.90 |
| Von Mises (b) | 1 | 37.60 | 50.43 | 46.57 | 38.33 |
| | 2 | 42.30 | 44.57 | 43.43 | 45.53 |
| | 3 | 53.83 | 38.73 | 43.73 | 49.87 |

The spread (delta) of the mean response across the three levels of each factor indicates its relative influence. For the von Mises failure response, the plate thickness (B) and concrete grade (C) produce the largest spreads, followed by the stirrup spacing (A), while the reinforcement material (D) produces the smallest change confirming that the reinforcement type is the least influential of the four factors. The same ranking is visible in the main-effect plots of Figures 5–8, where the lines for factor D are the flattest. This ordering is physically reasonable, because the tube thickness and the concrete grade directly control the confinement and load-sharing that govern the failure stress of a CFST member. (Fig. 5 to 8)

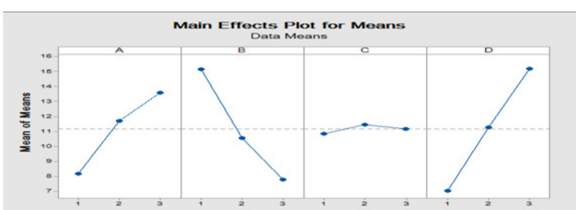


Figure 5: Main-effect plot of the mean response for the displacement along the Z-axis

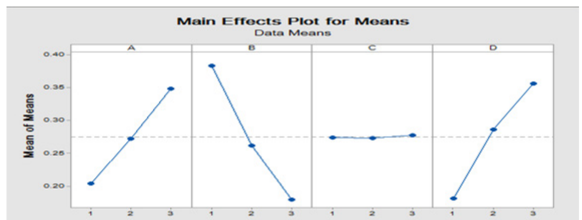


Figure 6: Main-effect plot of the mean response for the displacement along the X-axis (column buckling)

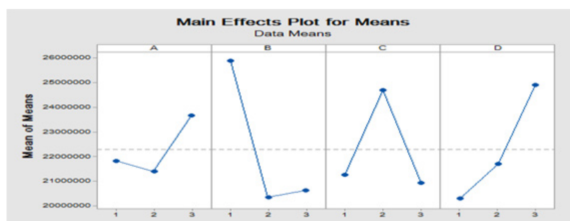


Figure 7: Main-effect plot of the von Mises failure response for series (a)


Figure 8: Main-effect plot of the von Mises failure response for series (b)

From the S/N plot of the von Mises failure response of series (a), the optimal level of each factor is A2, B2, C3, D1: a stirrup spacing at the second level (6 cm), plate thickness at the second level, concrete grade at the third level (35 MPa) and reinforcement at the first level (steel). Consequently, a CFST column with medium plate thickness, maximum concrete strength and steel reinforcement, loaded along the Z-axis, gives the lowest von Mises stress and the lowest probability of failure and buckling. The analysis further shows that stirrup spacing, concrete grade and plate thickness significantly influence column quality, whereas the reinforcement material is almost ineffective (Lee & Wong, 2023; Zamir Hashmi et al., 2022).

## RESULTS AND CONCLUSION

The results confirm that geometry and material grade, rather than the reinforcement type, dominate the quality of the CFST column. The pronounced effect of concrete grade and plate thickness reflects the confinement mechanism at the heart of CFST behaviour: a higher-grade core and an appropriately thick tube enhance the triaxial confinement and delay local buckling, lowering the von Mises stress under axial load (Han et al., 2014; Li et al., 2024). The comparatively small influence of the reinforcement material on the failure response despite its clear effect on ductility and energy absorption is consistent with FRP-confined and recycled-aggregate CFST studies, in which the outer confinement and core strength govern peak capacity while the reinforcement mainly modifies post-peak behaviour (Zeng et al., 2022; Liang et al., 2021; Zhu et al., 2023). The identified optimum (A2B2C3D1) therefore represents a balanced design in which a moderate stirrup spacing and plate thickness combine with the strongest concrete and a steel cage to minimise failure stress. From a practical standpoint, the coupled Taguchi–finite-element procedure reduced a prohibitively large full-factorial study (which would require many more analyses) to nine simulations while still ranking the parameters and locating the optimum, illustrating the efficiency of design-of-experiments methods for composite-column design (Anwar et al., 2022; Mawlood & Rafiq, 2022). The study is nevertheless bounded by its scope: a single circular geometry, three levels per factor, and monotonic loading in two directions. Extending the array to more factors and levels, incorporating cyclic and long-term loading, and validating against a dedicated experimental programme would further strengthen the conclusions and are proposed as future work. Therefor:

•CFST columns show remarkable capability and efficiency because of the complementary properties of steel and concrete; the concrete core delays local buckling of the steel wall, so a suitable steel-beam-to-CFST-column connection allows these benefits to be fully exploited.

•To verify the ANSYS results, a laboratory model of a concrete column enclosed by a steel plate and stirrups was selected, and its results agreed closely with the finite-element model.

•The load–displacement curves from the non-linear analysis show that the reinforcement material significantly affects the system response; the highest energy absorption and ductility occur with CFRP reinforcement, whereas the maximum ultimate strength occurs with steel reinforcement.

•From the stress contours, the steel plate yields at the lower part of the column because of the high moment there.

•The S/N analysis of the von Mises failure response of series (a) gives the optimal combination A2B2C3D1, 6 cm stirrup spacing, medium plate thickness, 35 MPa concrete and steel reinforcement which yields the lowest von Mises stress and the lowest failure and buckling probability.

•Comparing the optimal state through Minitab and the L9 orthogonal array confirmed that the accuracy of the systematic Taguchi design method is very appropriate for optimising CFST-column parameters.

## REFERENCES


*Al-Abbas, B., Abdul Rasoul, Z. M. R., Hasan, D., & Rasheed, S. E. (2023). Experimental study on the ultimate strength of a steel tube column filled with reactive powder concrete. Civil Engineering Journal, 9(6), 1344–1355.* https://doi.org/10.28991/CEJ-2023-09-06-04

*Al-Rousan, R., Nusier, O., Abdalla, K., Alhassan, M., & Lagaros, N. D. (2022). NLFEA of sulfate-damaged circular CFT steel columns confined with CFRP composites and subjected to axial and cyclic lateral loads. Buildings, 12(3), 296.* https://doi.org/10.3390/buildings12030296

*Anwar, F. H., El-Hassan, H., Hamouda, M., El-Mir, A., Mohammed, S., & Mo, K. H. (2022). Optimization of pervious geopolymer concrete using the TOPSIS-based Taguchi method. Sustainability, 14(14), 8767.* https://doi.org/10.3390/su14148767

*Beck, J., & Kiyomiya, O. (2003). Fundamental pure torsional properties of concrete-filled circular steel tubes. Journal of Materials, Concrete Structures and Pavements, JSCE, 2003, 285–296.*

*Belal, M. F., Mohamed, H. M., & Morad, S. A. (2014). Behavior of reinforced concrete columns strengthened by steel jacket. HBRC Journal, 11(2), 201–212.*

*Chen, C. C., & Lin, N. J. (2006). Analytical model for predicting axial capacity and behavior of concrete encased steel composite stub columns. Journal of Constructional Steel Research, 62(5), 424–433.*

*Du, P., Yang, Y., & Tan, K. H. (2022). Effects of biaxial bending and axial restraint on hybrid fibre-reinforced high-performance concrete columns at elevated temperatures. Journal of Structural Engineering, 148(12), 04022185.* https://doi.org/10.1061/(ASCE)ST.1943-541X.0003484

*Ellobody, E., Young, B., & Lam, D. (2011). Eccentrically loaded concrete encased steel composite columns. Thin-Walled Structures, 49(1), 53–65.*

*Gao, H. Y., Wang, L. G., Chen, B. L., & Li, X. (2022). Experimental investigation on the flexural performance of splicing GFRP–concrete–steel sandwich composite members. Advances in Structural Engineering, 25(15), 3155–3170.* https://doi.org/10.1177/13694332221119875

*Han, L. H., Huang, H., Tao, Z., & Zhao, X. L. (2006). Concrete-filled double-skin steel tubular (CFDST) beam-columns subjected to cyclic bending. Engineering Structures, 28(12), 1698–1714.*

*Han, L. H., Li, W., & Bjorhovde, R. (2014). Developments and advanced applications of concrete-filled steel tubular (CFST) structures: Members. Journal of Constructional Steel Research, 100, 211–228.* https://doi.org/10.1016/j.jcsr.2014.04.016

*Han, T. H., Han, K. H., Han, S. Y., Kim, S. N., Kang, J. O., & Kang, Y. J. (2005). The behavior of an internally confined hollow concrete-filled steel tube column. In Proceedings of the 8th Korea–Japan joint seminar on steel bridges.*

*Jayaganesh, S., Raja, M. J., Ganesh, P. G., & Jegan, J. (2015). Effects of concentrical partial (local) compression on the structural behavior of concrete-filled steel tubular columns. Advances in Materials Science and Engineering, 2015, 491038.* https://doi.org/10.1155/2015/491038

*Lee, K. J. L., & Wong, S. F. (2023). Multi-objective Taguchi optimization of cement concrete incorporating recycled mixed plastic fine aggregate using a modified Fuller's equation. Buildings, 13(4), 893.* https://doi.org/10.3390/buildings13040893

*Li, G., Hou, C., & Shen, L. (2021). Life-cycle analysis of FRP-strengthened offshore CFST columns suffering from steel corrosion. Composite Structures, 277, 114607.* https://doi.org/10.1016/j.compstruct.2021.114607

*Li, X., Zhang, S., Tao, Y., & Zhang, B. (2024). Numerical study on the axial compressive behavior of steel-tube-confined concrete-filled steel tubes. Materials, 17(1), 155.* https://doi.org/10.3390/ma17010155

*Liang, J. F., Lin, S. Q., & Ahmed, M. (2023). Axial behavior of carbon-fibre-reinforced-polymer-confined recycled-aggregate concrete-filled steel tube slender square columns. Scientific Reports, 13, 10075.* https://doi.org/10.1038/s41598-023-37101-4

*Liang, J. F., Lin, S. Q., Li, W., & Liu, D. W. (2021). Axial compressive behavior of recycled-aggregate concrete-filled square steel tube stub columns strengthened by CFRP. Structures, 29, 1874–1881.* https://doi.org/10.1016/j.istruc.2020.12.084

*Liao, J., Zeng, J., Quach, W. M., & Zhou, J. K. (2023).*

*Axial compressive behavior and model assessment of FRP-confined seawater sea-sand concrete-filled stainless-steel tubular stub columns. Composite Structures, 311, 116782. https://doi.org/10.1016/j.compstruct.2023.116782*

*Lubliner, J., Oliver, J., Oller, S., & Oñate, E. (1989). A plastic-damage model for concrete. International Journal of Solids and Structures, 25(3), 299–326. https://doi.org/10.1016/0020-7683(89)90050-4*

*Mander, J. B., Priestley, M. J. N., & Park, R. (1988). Theoretical stress-strain model for confined concrete. Journal of Structural Engineering, 114(8), 1804–1826. https://doi.org/10.1061/(ASCE)0733-9445(1988)114:8(1804)*

*Mawlood, D., & Rafiq, S. (2022). Nonlinear 3D finite-element model for round composite columns under various eccentricity loads. Engineering and Technology Journal, 40(11), 1605–1614. https://doi.org/10.30684/etj.2022.133106.1168*

*Schneider, S. P. (1998). Axially loaded concrete-filled steel tubes. Journal of Structural Engineering, 124(10), 1125–1138. https://doi.org/10.1061/(ASCE)0733-9445(1998)124:10(1125)*

*Shakir-Khalil, H., & Illouli, S. (1987). Composite columns of concentric steel tubes. In Proceedings of the conference on the design and construction of non-conventional structures. Civil-Comp Press.*

*Shanmugam, N. E., & Lakshmi, B. (2001). State of the art report on steel-concrete composite columns. Journal of Constructional Steel Research, 57(10), 1041–1080.*

*Tao, Z., Han, L.-H., & Zhao, X.-L. (2004). Behaviour of concrete-filled double-skin (CHS inner and CHS outer) steel tubular stub columns and beam-columns. Journal of Constructional Steel Research, 60(8), 1129–1158.*

*Tarabia, A. M., & Albakry, H. F. (2014). Strengthening of RC columns by steel angles and strips. Alexandria Engineering Journal, 53(3), 615–626.*

*Wei, S., Mau, S. T., Vipulanandan, C., & Mantrala, S. K. (1995). Performance of a new sandwich tube under axial loading: Experiment. Journal of Structural Engineering, 121(12), 1806–1814.*

*Yu, T., Teng, J. G., & Wong, Y. L. (2010). Stress-strain behavior of concrete in hybrid FRP-concrete-steel double-skin tubular columns. Journal of Structural Engineering, 136(4), 379–389.*

*Zamir Hashmi, S. R., Khan, M. I., Khahro, S. H., Zaid, O., Shahid Siddique, M., & Md Yusoff, N. I. (2022). Prediction of the strength properties of concrete containing waste marble aggregate and stone dust – modeling and optimization using RSM. Materials, 15(22), 8024. https://doi.org/10.3390/ma15228024*

*Zeng, J.-J., Liao, J., Liang, W.-F., Guo, Y.-C., Zhou, J.-K., Lin, J.-X., & Yan, K. (2022). Cyclic axial compression behavior of FRP-confined seawater sea-sand concrete-filled stainless-steel tube stub columns. Frontiers in Materials, 9, 872055. https://doi.org/10.3389/fmats.2022.872055*

*Zeng, J. J., Zhu, D. H., Liao, J., Zhuge, Y., Bai, Y. L., & Zhang, L. (2022). Large-rupture-strain FRP-confined concrete in square columns: Effects of specimen size and assessment of existing models. Construction and Building Materials, 327, 126869. https://doi.org/10.1016/j.conbuildmat.2022.126869*

*Zhao, X. L., & Grzebieta, R. (2002). Strength and ductility of concrete-filled double-skin (SHS inner and SHS outer) tubes. Thin-Walled Structures, 40(2), 199–213.*

*Zhao, X. L., & Han, L. H. (2006). Double-skin composite construction. Progress in Structural Engineering and Materials, 8(3), 93–102.*

*Zhao, X. L., Grzebieta, R. H., & Elchalakani, M. (2002). Tests of concrete-filled double-skin CHS composite stub columns. Steel and Composite Structures, 2(2), 129–146.*

*Zhou, J. (1990). Experimental research on concrete-filled steel tubular slender columns under combined compression and torsion (Master's thesis). Beijing Institute of Civil Engineering and Architecture. [in Chinese]*

*Zhu, D. H., Zhong, G. Q., Zeng, J. J., & Liao, J. (2023). Behavior and model evaluation of large-rupture-strain FRP-confined concrete-encased high-strength steel columns under axial compression. Thin-Walled Structures, 183, 110367. https://doi.org/10.1016/j.tws.2022.110367*

*Abdulkhudhur, R., Al-Quraishi, H., & Elwi, M. (2024). Numerical analysis of concrete-encased concrete-filled steel tube beams. AIP Conference Proceedings, 3219(1), 020018. https://doi.org/10.1063/5.0236329*

*Bai, Y. L., Mei, S. J., Chan, C. W., & Li, Q. Q. (2021).*

*Compressive behavior of large-size square PEN FRP-concrete-steel hybrid multi-tube concrete columns. Engineering Structures, 246, 113017.* https://doi.org/10.1016/j.engstruct.2021.113017

*Guo, S., Xiao, S. H., Shi, H. W., Zeng, J. J., Wang, W. Q., & Zhao, H. C. (2020). Axial compressive behavior of concrete-filled FRP-steel wire reinforced thermoplastics pipe hybrid columns. Composite Structures, 244, 112237.* https://doi.org/10.1016/j.compstruct.2020.112237

COPYRIGHTS

©2023 The author(s). This is an open access article distributed under the terms of the Creative Commons Attribution (CC BY 4.0), which permits unrestricted use, distribution, and reproduction in any medium, as long as the original authors and source are cited. No permission is required from the authors or the publishers.

HOW TO CITE THIS ARTICLE

Azimi,M , Habibi,M R and Tavana ,M H . (2026). Optimization of CFST Column Parameters Employing the Taguchi Method and Finite Element Analysis. International Journal of Urban Management and Energy Sustainability, ( ), e738806

DOI: 10.22034/ijumes.2026.2096172.1386